Physical Aging in the Mechanical Properties of Miscible Polymer Blends

GENG-WEN CHANG,[1] ALEX M. JAMIESON,[1] ZHIBIN YU,[2] JOHN D. McGERVEY[2]

[1]Department of Macromolecular Science, Case Western Reserve University, Cleveland, Ohio 44106

[2]Department of Physics, Case Western Reserve University, Cleveland, Ohio 44106

Received 5 June 1996; Accepted 14 August 1996

ABSTRACT: Changes in mechanical properties during isothermal physical aging were investigated for three miscible blends: polystyrene (PS)/poly(2,6-dimethyl 1,4-phenylene oxide) (PPO), PS/poly(vinylmethylether) (PVME), and poly(methylmethacrylate) (PMMA)/poly(ethyleneoxide) (PEO). The kinetics of stress relaxation was investigated for the blend, dilute in one component, and compared with that of the neat major component at equal temperature distances, $T_g - T$, from the midpoint glass transition temperature. It is demonstrated that for all three blends, the mean stress relaxation time $\langle \tau \rangle$ does not scale with $T_g - T$. For PS/PPO and PS/PVME blends, the stress relaxation rates are faster compared to neat PS; for PMMA/PEO, they are slower than for neat PMMA. Two effects appear to be important in contributing to this discrepancy. First, addition of the second component produces a change in the packing density of the blend: less dense for PS/PPO and PS/PVME; more dense for PMMA/PEO. Comparison of average free volume hole sizes and fractional free volumes measured via orthopositronium annihilation lifetime measurements for all three blends versus the pure constituents are qualitatively consistent with this interpretation. Second, because of the presence of concentration fluctuations in the blend, it is expected that the initial stress decay is dominated by regions enriched in the more mobile component. From observations of the change in width of the stress relaxation time distribution, this effect appears to be particularly significant in the PS/PVME blend. J Appl Polym Sci **63:** 483–496, 1997

Key words: physical aging; stress relaxation; positron annihilation

INTRODUCTION

It is a well-known fact that changes in structure and materials properties occur in glassy polymers upon annealing below the glass transition temperature. This time-dependent behavior is often referred to as physical aging and is a direct consequence of the nonequilibrium nature of the glassy state. The significance of this phenomenon is that materials performance must be predictable to comply with design requirements throughout the service life of polymer products. It is thus important to be able to predict long-term properties from short-term tests. With regard to dynamic mechanical properties, such as creep and stress relaxation, a useful approach has been proposed by Struik,[1] and explored exhaustively by others.[2–4] This involves generating a master curve from repeated short-term dynamic tests during isothermal annealing, which yields aging shift factors that describe the kinetics of the physical aging process, namely, the slowing down of creep or stress relaxation with annealing time.

It is generally accepted that the change in dynamic mechanical properties arises from the densi-

Correspondence to: A. M. Jamieson

fication that occurs in the glass on annealing. This relationship is usually expressed in terms of the free volume concept. To permit the molecular motion that facilitates the dissipation of stress in the material (or the sample deformation in creep), a certain amount of unoccupied ("free") volume is necessary. On annealing, the level of free volume decreases, and molecular motion slows down. This picture is supported by recent experiments using spectroscopic probes whose characteristics are sensitive to the free volume of their local environment.[5–9] Since the materials properties of amorphous polymers are frequently interpreted in terms of the free volume concept, it is advantageous to have a spectroscopic technique by means of which quantitative information on free volume can be generated. During recent years, it has been established[10–18] that positron annihilation lifetime (PAL) spectroscopy is a useful method for such analysis both in the melt and glass. PAL spectroscopy involves measurement of the lifetime of positrons injected into a polymer sample from a positron-emitting nucleus, generally Na^{22}. There are three possible fates for such positrons: they can annihilate as free positrons, with a lifetime of the order $\tau_2 \sim 0.4$ ns; or they can form a transient bound state with an electron, termed positronium, in which the spins are either antiparallel, parapositronium (pPs), or parallel, orthopositronium (oPs). The former has a very short lifetime, $\tau_1 = 0.125$ ns, the latter a very long lifetime, $\tau_3 \sim 1$ to 3 ns, whose magnitude increases with the size of the regions of low electron density (free volume holes) in which it forms. Frequently, in the interpretation of PAL experiments, it is assumed that the intensity of the oPs component of the PAL decay spectrum, I_3, which is proportional to the probability of oPs formation, is a measure of the number density of holes.[10–18] Also, from the oPs lifetime, the average hole radius R can be determined from the following theoretical equation:

$$\tau_3^{-1} = 2[1 - R/R_o + \tfrac{1}{2\pi} \sin(2\pi R/R_o)] \quad (1)$$

Here, $\Delta R = R_o - R$ is the width of the interface between the hole and the bulk electron density. From experimental results on various molecular solids, it has been determined that $\Delta R = 0.1656$ nm. We have established[12–18] a quantitative correspondence between independent estimates of fractional free volume in amorphous polymers and a fractional free volume determined from PAL analysis, h_{pos}, in the form:

$$h_{pos} = CI_3\langle v_h \rangle \quad (2)$$

where $\langle v_h \rangle$ is the average hole volume determined as $\langle v_h \rangle = (4\pi/3)R^3$, and C is an empirical constant.

The formulation of polymer blends is a useful approach to produce materials whose properties are a combination of those of the blend constituents. The physical aging behavior of miscible blends in the glassy state has been investigated,[19–21] and it is observed that the time evolution of dynamic mechanical properties during isothermal annealing is similar to that of the pure components, albeit at a different, typically intermediate, rate. It is of interest to determine whether there are simple temperature scaling laws for the rate of physical aging phenomena in such systems. This would facilitate efforts to develop a molecular theory for the kinetics of aging in miscible blends. In this respect, the glass transition temperature would appear *a priori* to be the most obvious scaling variable. A ubiquitous feature of the glass transition region of miscible blends, however, is that it is typically wider than that of the blend components. This phenomenon has been interpreted[23] as being due to the presence of concentration fluctuations in the blend,[24] which give rise to a range of microenvironments at which the local glass transition varies depending on the composition. Such microheterogeneities may influence dynamic mechanical behavior, the early stages of which are likely to be dominated by the motions of relaxing elements in the more mobile regions. Thus, when comparing the kinetics of creep or stress relaxation of different blend compositions, or of blends versus the pure components, it may be more relevant to use a temperature located below the usual midpoint value, T_g, defined in Figure 1, as the scaling variable.

In this paper, we evaluate the role of concentration fluctuations, and of changes in free volume, on the kinetics of stress relaxation during isothermal physical aging in miscible polymer blends. To do this, we utilize blends that are dilute in one component and compare the rates of tensile stress relaxation in such blends versus those of the neat major component in the glassy state at equal temperature distances $T_g - T$ from the mid-point T_g. In addition, we carry out orthopositronium annihilation lifetime measurements of free volume as a basis for interpreting the stress relaxation behavior of these materials.

EXPERIMENTAL

Materials

Polystyrene (PS), poly(vinyl methyl ether) (PVME), poly(methylmethacrylate) (PMMA),

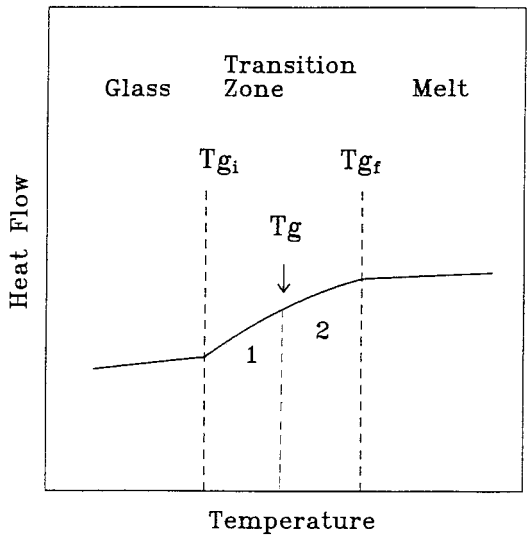

Figure 1 Schematic illustration showing the broadening of the glass transition region in the DSC trace due to concentration fluctuations and defining the initial, final, and mid-point transition temperatures T_{gi}, T_{gf}, and T_g.

and poly(ethylene oxide) (PEO) were purchased from Scientific Polymer Products, Inc., and poly-(2,6 dimethyl 1,4 phenylene oxide) (PPO) from Polyscience. Details of molecular characterization of these polymers are given in Table I. Blends with wt/wt compositions dilute in one component were prepared by solvent casting on clean glass slides. 90/10 PS/PPO and 85/15 PMMA/PEO were cast from 5% wt/vol solution in chloroform, and 90/10 PS/PVMe from 5% wt/vol solution in toluene. The solvent-cast films were annealed under vacuum at ambient temperature for two days and then at 65°C for 72 h to remove all solvent. The films were molded at 40°C above their glass transition temperatures to obtain square sheets with a thickness of 1 mm. Similar specimens were prepared for pure PS, PMMA, and PPO by directly molding the as-received materials, also at T_g + 40°C. Standard ASTM D 1708-84 dog-bone-shaped specimens and small discs of 8 mm radius were cut from the molded sheets by blade die. The former were utilized in stress relaxation experiments, the latter in positron annihilation analyses. These specimens were stored in a sealed dessicator to prevent any moisture uptake when not being used.

Methods of Procedure

Differential Scanning Calorimetry

The glass transition temperatures of blends and homopolymers were determined using a Perkin Elmer Differential Scanning Calorimeter 7 at a heating rate of 20°C/min. Each differential scanning calorimetry (DSC) testing cycle consisted of heating, cooling, and repeat heating scans. The first heating scan provides a rough estimate of T_g; the highest temperature in the transition region was then chosen as the annealing temperature, and the sample was annealed at this temperature for three minutes to eliminate prior thermal history. The final heating scan was performed immediately after cooling (at 100°C/min) from the annealed state. The T_g of the sample was determined from this final scan as the point of equidistance from the baseline, above and below the transition zone, as indicated in Figure 1. This T_g value was subsequently used as the reference temperature in selecting the aging temperatures for stress relaxation experiments. For the purposes of later analysis, we further determined the onset and terminal glass transition temperatures, $T_{g,i}$ and $T_{g,f}$, as shown also in Figure 1. The particular thermal history for DSC measurements described above was chosen to facilitate definition of a tempera-

Table I Materials Characteristics

Polymer	M_w	M_w/M_n	T_{gi}[a]	T_g[a]	T_{gf}[a]
Polystyrene	280,000	1.75	100	105	110
Polyphenyleneoxide	41,000	1.95	208	212	216
PS/PPO (90/10)	—	—	107	116	125
Polyvinylmethylether	98,500	2.07	—	—	—
PS/PVME (90/10)	—	—	54	72	90
Polymethylmethacrylate	400,000	1.43	105	112	119
Polyethyleneoxide	180,000[b]	—	—	—	—
PMMA/PEO (85/15)	—	—	52	67	82

[a] Measured by DSC at a heating rate of 20°C/min.
[b] Viscosity-average molecular weight.

ture reference scale when comparing the properties of blends and homopolymers in the glassy state. Results for T_g, $T_{g,i}$, and $T_{g,f}$ are summarized in Table I. We found that the width of the glass transition region was $dT_g = T_{gf} - T_{gi} = 8$°C for PPO, 9°C for PS, 15°C for PMMA, 18°C for PS/PPO, 35°C for PS/PVME, and 35°C for PMMA/PEO. Finally, with regard to the 85/15 PMMA/PEO blend, we note that the DSC thermogram showed no trace of a melting transition for PEO, i.e., no evidence of the presence of crystalline PEO.

Tensile Stress Relaxation

The variation of stress relaxation at small strains under simple tensile extension was probed sequentially during isothermal annealing in the glass. These experiments were performed using a Rheometrics Solids Analyser II (RSA II) equipped with a temperature-controlled testing chamber. The RSA II is a microprocessor-controlled tensile testing instrument featuring air-bearing transducers which reduce the stress-strain response time to less than 5 ms. The sample temperature is controlled to within ±0.5°C throughout the duration of measurements (max. 9 h). Sample temperature is measured by a thermocouple positioned at the center of the dog bone.

The testing sequence for stress relaxation measurements during isothermal annealing was chosen to conform to the schedule suggested by Struik,[1] which consists of alternate aging and measuring periods. The samples were first annealed at T_g + 10°C in the test chamber to erase previous thermal history and reach thermal equilibrium. This was followed by a quench to the aging temperature, T_a, by blowing cold, dry air into the chamber. The time required to cool the specimen from T_g + 10°C to T_a was typically two minutes. The alternative of a faster quench in liquid nitrogen was rejected because such a high cooling rate might introduce internal stresses in the samples.

The time at which the sample reached the aging temperature was designated zero aging time, $t_a = 0$. Successive tensile stress relaxation tests were carried out at different aging times (t_a). During each test, the sample was kept at a constant strain (0.2%), and the stress was monitored until the testing time approached 10% of the aging time. This ensures that aging effects during individual tests are negligible. Results were recorded as the tensile stress modulus (N/m^2):

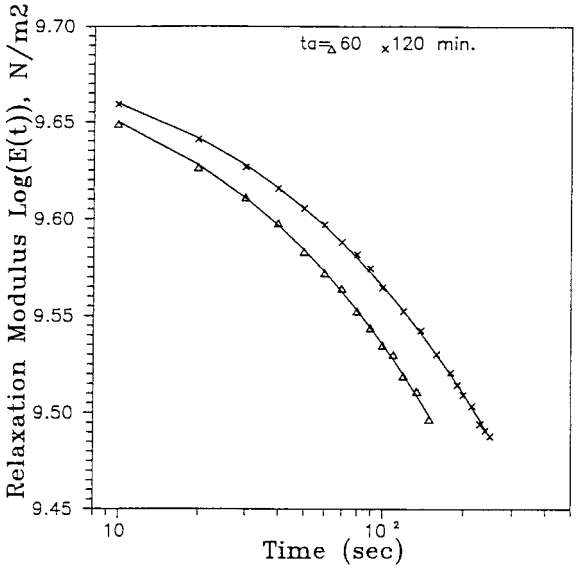

Figure 2 Stress relaxation curves for PS/PPO (90/10) blend during isothermal aging at $T_a = T_g - 20$°C and $t_a = 1$ h and $t_a = 2$ h following a quench from the equilibrium melt above T_g. Solid lines are least squares fits to the initial data, and the symbols represent repeat tests to demonstrate thermoreversibility.

$$E(t) = \sigma(t)/\varepsilon \tag{3}$$

where $\sigma(t)$ is the stress recorded by the RSA II, and the strain applied is $\varepsilon = 0.2\%$. At the end of each measurement, the strain was released, and the sample was maintained at the aging temperature. Aging experiments were carried out at several different temperatures for each blend and homopolymer in the glassy state. In Figure 2 (Figs. 3–12), we show examples of the reproducibility of individual stress relaxation tests, under equivalent isothermal aging conditions (t_a = 60 min and t_a = 120 min) following a quench from the equilibrium melt. This experiment was performed on a glassy film prepared from a blend of 10% PPO in PS. The stress relaxation curve can be well described by a stretched exponential expression of the form[1–4]:

$$E(t)/E_o = \exp(-(t/\tau)^{\beta}) \tag{4}$$

Thus, in Figure 2, we overlay repeat experimental data (symbols) on the fits to previous experiments via eq. (4) (solid lines). Clearly, the reproducibility is very good. Note that, in eq. (4), τ is a characteristic relaxation time, and the exponent β characterizes the width of the relaxation spectrum in the sense that the width increases as β decreases from a value of unity (single exponential decay).

Also, the average stress relaxation time can be computed as $\langle\tau\rangle = (\tau/\beta)\Gamma(1/\beta)$.

Positron Annihilation Lifetime (PAL) Spectroscopy

In PAL spectroscopy, we characterize the statistics of the time interval between detection of the 1.28 MeV gamma ray, which accompanies the emission of a positron by the Na^{22} source, and the 0.511 MeV gamma rays, which are produced on annihilation in the polymer specimen. The instrument used in this work has been thoroughly described in previous articles,[12–18] and consists of BaF_2 and CsF gamma ray detectors, a fast-fast coincidence system based on EG&G Ortec MIN modules (model 583 constant-fraction discriminators) and a model 566 time-to-amplitude converter. A cylindrical CsF crystal (1.5 in. length; 1.5 in. diameter) coupled to a photomultier tube (Hamamatsu, type H2431) is used as a scintillator to record the 1.28 MeV positron birth signal and a conical BaF_2 crystal (0.8 and 1.0 in. diameter; 1.0 in. length), likewise mounted to a Hamamatsu H2431Q phototube, records one of the 0.511 MeV "death" signals. Positron lifetime spectra were collected on a PCA multichannel analyzer (Nucleus Inc.).

Disc-shaped film samples with 8 mm radius were stacked to 2 mm thickness, the radiation source ^{22}Na (25 μCi) was sandwiched between two 2 mm stacked discs, and the sandwich mounted in a copper sample holder enclosed within a vacuum chamber. All specimens for PAL spectroscopy were cut from the same sample sheet used for mechanical studies. The source was deposited on thin aluminum foil (1.7 mg/cm^2) within an area of diameter 2.5 mm. Sample temperature was maintained to within ± 0.2°C by means of two diode sensors connected to a temperature controller (Lake Shore Cryogenics, model 805).

PAL spectra were fit to a sum of four exponential decays and convoluted with a resolution function, by means of the program PATFIT-88.[25] The resolution function was approximated as a sum of three Gaussians whose statistical weights and widths at half maximum (FWHM) are determined by the fitting program. The resolution function consistently had a FWHM of 0.23 ns equal to that measured directly using a ^{60}Co source. The analysis yields the common starting position t_o and the four intensities (I_s, I_1, I_2, I_3), and four decay constants (τ_s, τ_1, τ_2, τ_3) for each exponential decay. In this fit, I_s, the number of positrons annihilating in the aluminum foil, is calculated from the known foil thickness to be 7%, the positron lifetime in aluminum is known to be $\tau_s = 0.18$ ns, and the p-Ps lifetime is known to be $\tau_1 = 0.125$ ns. The reader is directed to our earlier articles, particularly Kluin et al.,[13] for more details of the analytical procedures for PAL spectroscopy.

RESULTS AND DISCUSSION

Stress Relaxation During Physical Aging

Momentary stress relaxation curves were obtained for polymers and their blends during isothermal physical aging at several temperatures in the glass, following a quench from the equilibrium melt, as illustrated in Figure 2. Typically, data were recorded at four aging times and fit to the stretched exponential expression, eq. (4), using a nonlinear least-squares Marquardt–Levenburg algorithm,[26] with an initial value E_o obtained from the first data point. The resulting β values were found to lie within a narrow range. An average value of β was then assumed, and values of E_o and τ were recalculated via the same fitting algorithm. From the excellent fits, it was found in general that an average β value is adequate to describe the stress relaxation process during short-term isothermal physical aging. Note that the question of whether β should remain constant during aging is controversial. Matsuoka et al.[27] argue that, as aging proceeds, β indeed remains invariant; Rendell et al.[28] and Yee et al.[29] conclude that β decreases, while Simha et al.[30] find that β increases. We typically observed a small systematic decrease in β as aging time increased. Our approach, however, is to use the data reduction with fewest floating parameters (i.e., constant β), which is consistent with the results within experimental error. Note that release of the constraint of constant β does not alter the conclusions of our experiments, as discussed later, in terms of the temperature scaling of the stress relaxation time distribution. Since β can be assumed invariant during aging, the momentary stress relaxation curves can be superposed by horizontal shifts along the logarithmic time axis, thus generating a master curve at an appropriately chosen reference time. Master curves constructed in this way are shown in Figure 3 for PS, PPO, and a PS/PPO blend at a weight composition ratio of 9 : 1. Each represents the superposition of stress relaxation data at aging temperatures $T_a = T_g - 20$, where T_g is the mid-point T_g, and at aging times $t_a = 30$,

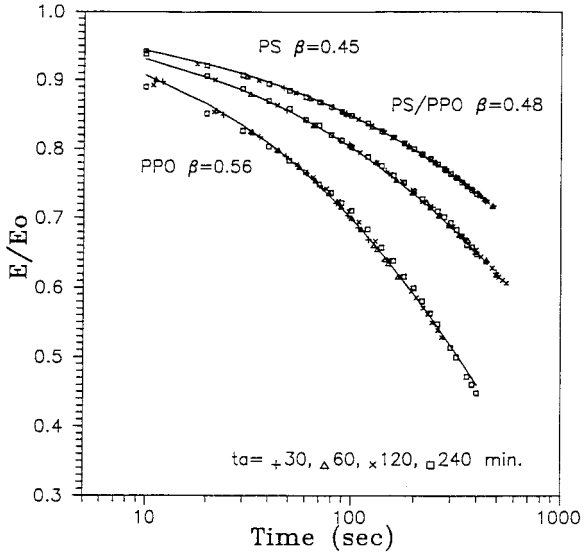

Figure 3 Superposition of stress relaxation curves for PS, PPO, and PS/PPO (90/10) blend at different aging times (t_a) and aging temperature $T_a = T_g - 20$°C. The reference curve was selected at $t_a = 4$ h. Solid lines are stretched exponential fits with exponents β indicated.

60, 120, and 240 min, with $t_a = 240$ min as the reference curve. Clearly, the rate of stress relaxation is faster in PPO than in PS at equal temperature distances from T_g. Also, the stress relaxation spectrum of PPO is narrower than that of PS, as manifested by the larger β value. The stress decay of the blend is closer to that of PS than PPO, as is expected since PS is the major component.

Similar experiments were conducted at aging temperatures $T_a = T_g - 15$, $T_g - 25$, and $T_g - 30$. The fit parameters, E_o, β, and τ and the mean relaxation times $\langle\tau\rangle$ for all four aging temperatures are summarized in the Tables II–IV. In Figure 4, values of $\langle\tau\rangle$ at aging reference time $t_a = 240$ min are plotted against temperature distance $T_g - T$, and compared with literature data of Ho et al.[21] The latter are numerically comparable to our results and show similar trends in that PPO relaxes faster than PS, though the difference is smaller. In contrast to our results, Ho et al. found a universal value of $\beta = 0.41$. Note that the data from Ho et al. shown in Figure 4 were collected 5 min after the start of stress relaxation using an Instron Tensile Tester, and the blend data selected from that study correspond to a PPO/PS composition of 80/20, which is closest to our value.

In comparing the behavior of the 90/10 PS/PPO blend versus pure PS, and recalling that the shape of the stress decay is very similar in both, we now attempt to evaluate how much of the difference in the scaling of $\langle\tau\rangle$ with respect to $T_g - T$ is due to the influence of concentration fluctuations in the blend. Certainly, $\langle\tau\rangle$ represents, in principle, an average over the entire stress relaxation process; but recall that we calculate it using values of τ and β based on a stretched exponential fit to the initial decay. We consider the idea[23,24] that the widening of the glass transition zone in the blend is due to the fact that, locally, there are regions richer in PS and others richer in PPO than the mean composition (90/10). The former have their local T_g values between T_{gi} and T_g; the latter between T_g and T_{gf}. We assume that it is molecular motion in the more mobile regions that determine the initial rate of stress relaxation in the glass and, therefore, that a temperature located between T_{gi} and T_g may be a better choice of scaling variable than the mid-point T_g. In Figure 5, we utilize the initial value T_{gi} as the scaling temperature and find that indeed there is a closer superposition of the $\langle\tau\rangle$ values for PS and PS/PPO than in Figure 4. This suggests to us that the faster rate of stress relaxation in the glass can be at least partly attributed to the existence of concentration-rich regions. In addition, a significant contribution must come from an increase in free volume introduced by the added PPO. Support for this interpretation is presented below in the form of free volume values obtained from o-Ps annihilation data.

It is also of interest to comment on the experimental values of the β parameter in Tables II–IV. As noted earlier, variations in β may be interpreted as indicating differences in the width of the stress relaxation time spectrum. These may be interpreted in terms of changes in the degree of cooperativity of the molecular motion in the polymer matrix. Central to the idea that mobility in amorphous polymers is controlled by free volume is the notion that if a particular chain segment is to move, neighboring segments must be displaced to accommodate the move, i.e., there is a coupling between the relaxing element and the surrounding polymer matrix. A broadening of the relaxation time distribution indicates an increase in the strength of this coupling.[28] Thus, the observation that β decreases with increase of $T_g - T$ (Tables II–IV) indicates an increase in the degree of cooperativity as one goes deeper into the glassy state. This is consistent with theoretical models since, at lower temperature, the density increases, and one expects a stronger coupling between the relaxing elements.[28] Also, the values of β for the PS/PPO blend are larger than those of

Table II Stretched Exponential Curves Fitting Results for PS

T_a (°C)	t_a (min)	E_o ($\times 10^9$ Pa)	τ (s)	β	$\langle\tau\rangle$ (s)
T_g-15	30	2.88	511.9	0.47	1166.0
T_g-15	60	2.88	816.3	0.47	1859.0
T_g-15	120	2.91	1276.9	0.47	2908.5
T_g-15	240	2.90	2234.0	0.47	5088.6
T_g-20	30	2.91	1186.2	0.45	2985.4
T_g-20	60	2.93	1783.8	0.45	4489.4
T_g-20	120	2.95	3150.0	0.45	7927.9
T_g-20	240	2.96	5645.0	0.45	14207.2
T_g-25	30	2.97	2507.7	0.41	7748.9
T_g-25	60	2.97	4322.9	0.41	13357.9
T_g-25	120	3.98	8116.8	0.41	25081.1
T_g-25	240	3.02	14386.4	0.41	44454.3
T_g-30	30	2.94	5730.4	0.40	19442.9
T_g-30	60	2.96	8313.0	0.40	28205.6
T_g-30	120	2.99	12610.9	0.40	42788.1
T_g-30	240	2.99	25248.2	0.40	85665.8

the major component PS over the entire range of T_g. Two factors are expected to control the β value of the blend at a given temperature distance, $T_g - T$: first is the presence of concentration fluctuations, which will increase β over the pure polymer; second is any change in structure (free volume) which may, in principle, increase or decrease β, depending on the nature of the interaction between the blend components. For the PS/PPO blend, since β is larger than for pure PS, we infer that the latter effect is dominant, i.e., the added PPO increases the matrix free volume.

Finally, we note that the aging rates of the stress relaxation time, $\mu = d \log\langle\tau\rangle / d \log t_a$ are smaller than unity: for PS, μ = 0.7–0.9; for PPO, μ = 0.54–0.64; and for PS/PPO, μ = 0.68–0.75. Thus, the behavior of the blend is very similar to the major component, PS. According to the discussion of Struik,[1] the smaller μ value for PPO indicates molecular motion is less self retarding, i.e., there is a lesser degree of cooperativity, consistent with the fact that β is larger for PPO.

Next we turn to a comparison of stress relaxation during physical aging in a 90/10 PS/PVME

Table III Stretched Exponential Curves Fitting Results for PPO

T_a (°C)	t_a (min)	E_o ($\times 10^9$ Pa)	τ (s)	β	$\langle\tau\rangle$ (s)
T_g-15	30	3.47	214.1	0.58	337.0
T_g-15	60	3.57	302.8	0.58	476.6
T_g-15	120	3.72	428.2	0.58	674.0
T_g-15	240	3.85	605.5	0.58	953.2
T_g-20	30	3.58	372.4	0.56	617.0
T_g-20	60	3.69	563.6	0.56	903.6
T_g-20	120	3.79	798.3	0.56	1322.9
T_g-20	240	3.92	1168.8	0.56	1936.9
T_g-25	30	3.70	448.9	0.50	897.8
T_g-25	60	3.74	680.3	0.50	1360.8
T_g-25	120	3.92	1031.3	0.50	2062.6
T_g-25	240	4.04	1563.1	0.50	3126.2
T_g-30	30	3.87	598.9	0.46	1415.2
T_g-30	60	3.93	790.2	0.46	2190.1
T_g-30	120	4.10	1222.8	0.46	3389.3
T_g-30	240	4.21	1892.4	0.46	5245.2

Table IV Stretched Exponential Curves Fitting Results for PS/PPO (90/10) Blend

T_a (°C)	t_a (min)	E_o ($\times 10^9$ Pa)	τ (s)	β	$\langle\tau\rangle$ (s)
T_g-15	30	4.89	368.1	0.47	831.0
T_g-15	60	4.92	548.4	0.47	1238.0
T_g-15	120	4.97	775.8	0.47	1751.3
T_g-15	240	4.93	1581.3	0.47	3569.7
T_g-20	30	5.03	463.7	0.48	978.9
T_g-20	60	5.07	692.8	0.48	1462.6
T_g-20	120	5.07	1035.9	0.48	2186.9
T_g-20	240	5.06	2282.3	0.48	4818.2
T_g-25	30	5.16	889.4	0.45	2173.4
T_g-25	60	5.19	1353.7	0.45	3308.0
T_g-25	120	5.27	1994.7	0.45	4847.5
T_g-25	240	5.17	4337.7	0.45	10600.3
T_g-30	30	5.12	1801.7	0.43	4908.8
T_g-30	60	5.17	2149.2	0.43	5855.6
T_g-30	120	5.24	3451.2	0.43	9402.9
T_g-30	240	5.23	5459.2	0.43	14873.8

blend with that of pure PS. The results of isothermal aging experiments on the blend at four annealing temperatures, $T_g - T$ = 15, 20, 25, and 30°C, analyzed by fits to eq. (4), are summarized in Table V. In Figure 6, we compare the stretched exponential master curves of E/E_o, scaled to aging reference time t_a = 240 min at $T_g - T$ = 20°C. These were generated for each material by procedures identical to those described above for PS/PPO. Comparing Table V to Table II, and clearly evident in Figure 6, we find that the relaxation rate of the PS/PVME blend is again faster than that of pure PS; however, the difference is much greater than in the case of PS/PPO (cf Fig. 3). Another distinguishing feature of PS/PVME from PS/PPO is that values of the β parameter of the blend are smaller than those of PS. Also, the aging rates μ for the blend are significantly smaller than those of PS. All of these observations can be rationalized by invoking a particularly strong in-

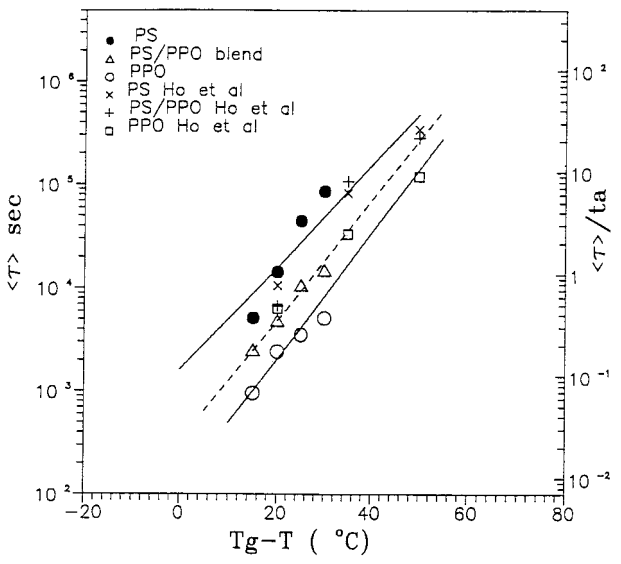

Figure 4 Mean stress relaxation times $\langle\tau\rangle$ are plotted against aging temperature distances $T_g - T$ for PS, PPO, and PS/PPO (90/10) blend at constant aging time t_a = 4 hours. Comparisons are made with the $\langle\tau\rangle$ data taken from Ho et al.[17]

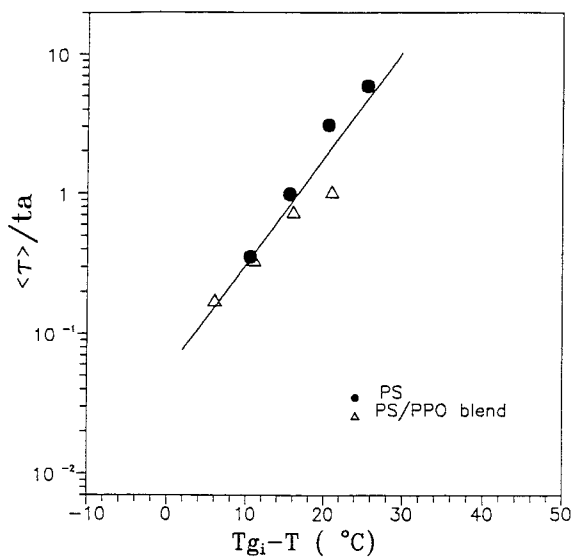

Figure 5 Improved scaling of $\langle\tau\rangle/t_a$ is obtained for PS/PPO (90/10) blend versus PS homopolymer by using $T_{gi} - T$ as the scaling variable rather than $T_g - T$.

Table V Stretched Exponential Curves Fitting Results for PS/PVME (90/10) Blend

T_a (°C)	t_a (min)	E_o ($\times 10^9$ Pa)	τ (s)	β	$\langle\tau\rangle$ (s)
T_g-15	30	3.00	66.5	0.39	237.4
T_g-15	60	2.96	86.6	0.39	309.1
T_g-15	120	2.77	125.2	0.39	446.9
T_g-15	240	2.85	149.0	0.39	531.8
T_g-20	30	3.26	225.4	0.38	850.9
T_g-20	60	3.29	322.5	0.38	1217.4
T_g-20	120	3.31	435.8	0.38	1645.1
T_g-20	240	3.28	637.8	0.38	2407.6
T_g-25	30	3.40	564.8	0.38	2230.7
T_g-25	60	3.57	822.4	0.38	3248.2
T_g-25	120	3.62	1095.6	0.38	4327.2
T_g-25	240	3.64	1620.2	0.38	6399.1
T_g-30	60	3.67	1656.5	0.37	6926.0
T_g-30	120	3.73	2362.3	0.37	9877.0
T_g-30	240	3.74	3625.5	0.37	15158.5

fluence of the concentration fluctuations on the stress relaxation behavior in the blend, consistent with the relatively broad glass transition region (Table I). Specifically, the large discrepancy in the temperature scaling of stress relaxation times $\langle\tau\rangle$ can again be substantially resolved by using T_{gi} as the scaling temperature, as shown in Figure 7. The smaller β value of the blend can be interpreted as reflecting the presence of microheterogeneities with a wide distribution of mobilities. The smaller values of μ in the blend are consistent with the well-known result that μ decreases as proximity to T_g increases (see Fig. 8).[1] Note that the experiments performed at the highest aging temperature, $T_g - T = 15$°C, are actually within the glass transition region of the blend. Again, it seems likely that a significant contribution to the faster stress relaxation in the blend comes from an increase in free volume from the added PVME, and this will be supported by o-Ps annihilation measurements described below.

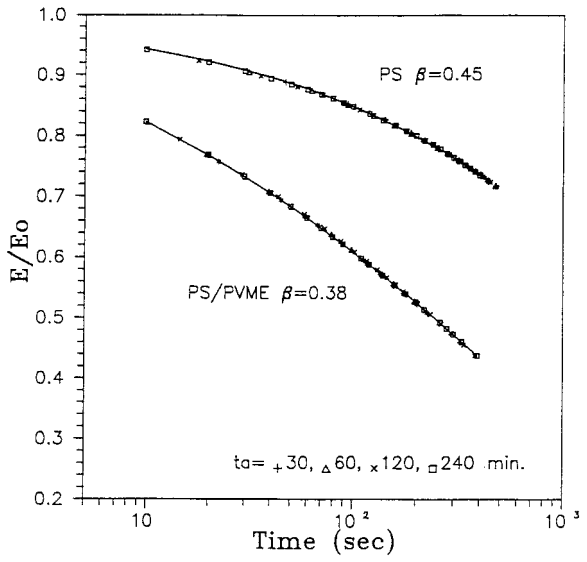

Figure 6 Superposition of stress relaxation curves for PS and PS/PVME (90/10) blend at different aging times (t_a) and aging temperature $T_a = T_g - 20$°C. The reference curve was selected at $t_a = 4$ h. Solid lines are stretched exponential fits with exponents β indicated.

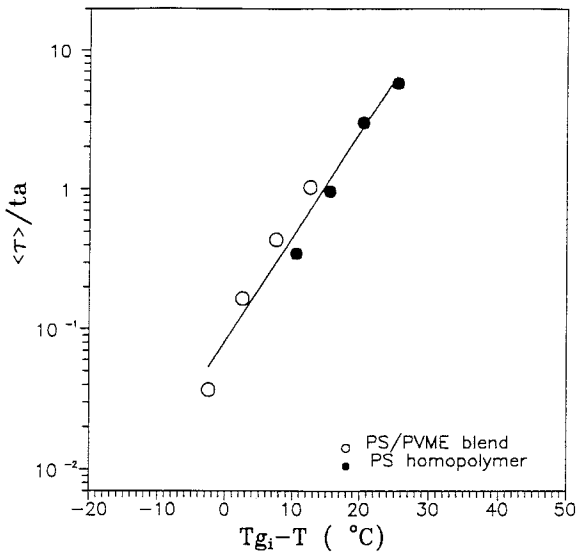

Figure 7 Approximate scaling of $\langle\tau\rangle/t_a$ values is obtained for PS/PVME (90/10) blend versus PS homopolymer is obtained using $T_{gi} - T$ as the scaling variable.

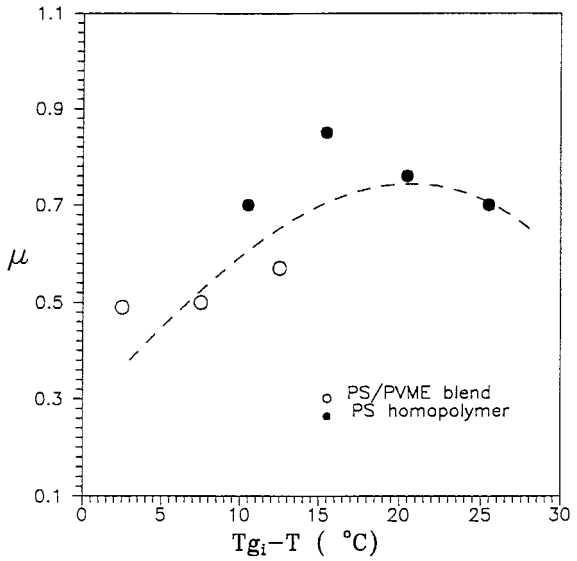

Figure 8 Temperature scaling of aging shift rate using $T_{gi} - T$ as the scaling variable.

Finally, we compare physical aging studies of stress relaxation in an 80/20 blend of PMMA/PEO with those in pure PMMA. The results of isothermal aging experiments on the blend at three annealing temperatures, $T_g - T = 7$, 17, and 27°C, analyzed by fits to eq. (4), are summarized in Table VII. Corresponding results on PMMA homopolymer at $T_g - T = 7$, 17, 27, and 37°C are given in Table VI. Stretched exponential master curves of blend and PMMA homopolymer, at aging temperature distance $T_g - T = 27$, are exhibited in Figure 9. Comparing Tables VI and VII, and from Figure 9, it is clear that the behavior of PMMA/PEO is dramatically different from the PS/PPO and PS/PVME blend systems in that the rate of stress relaxation in the blend is slower than in the PMMA homopolymer. Apparently, there is a large reduction in mobility in the PMMA/POE blend. Obviously, this situation is not resolved by invoking the presence of concentration fluctuations, e.g., by using T_{gi} as a scaling temperature. These observations suggest that the structure of the blend is altered in such a way that free volume is drastically reduced. Consistent with this, we note that, in the blend, the values of the β-parameter are smaller and the aging rates μ are larger, indicating a higher degree of cooperativity in the molecular motion, i.e., a stronger coupling between the relaxing segment and the surrounding matrix.[28] In this regard, it is interesting to note that, while a small-angle neutron scattering study[31] found that the radius of gyration of PMMA in PMMA/PEO blends is the same as in pure PMMA, Fourier transform infrared (FTIR) spectroscopy studies[32] indicate a change in conformation of the PEO from a helical to a trans planar structure. Also, rheological and rheooptical studies on PMMA/PEO blends in the melt report an increase in the viscoelastic relaxation times interpreted as due to increased monomeric friction coefficients of the two polymers.[33,34]

Positron Annihilation Spectroscopy

It is of interest to investigate whether any evidence exists for changes in free volume in the various blend systems as a basis to interpret the above stress relaxation observations. We present results of oPs annihilation lifetime measurements on each blend and on the corresponding homopolymers as a function of temperature in the glass. In discussing these data, we focus first on the oPs lifetimes τ_3 and the hole sizes R, computed from τ_3 via eq. (1), and then on estimates of the fractional free volume h, determined by combining τ_3 and I_3 values using eqs. (1) and (2). Note that interpretation of the latter could be influenced by the possibility that changes in I_3 between blend and homopolymer could reflect differences in oPs formation due to electronic effects rather than free volume.[35] Since oPs annihilation can clearly

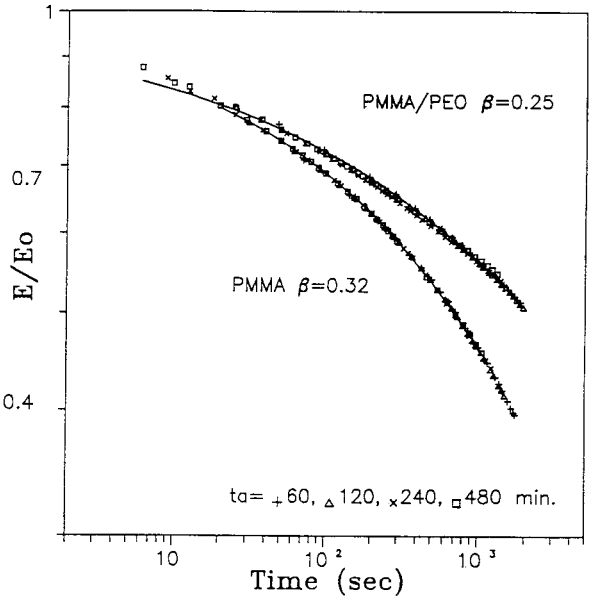

Figure 9 Superposition of stress relaxation curves for PMMA and PMMA/PEO (85/15) blend at different aging times (t_a) and aging temperature $T_a = T_g - 27$°C. The reference curve was selected at $t_a = 4$ hours. Solid lines are stretched exponential fits with exponents β indicated.

Table VI Stretched Exponential Curves Fitting Results for PMMA

T_a (°C)	t_a (min)	E_o ($\times 10^8$ Pa)	τ (s)	β	$\langle\tau\rangle$ (s)
T_g-7	60	0.44	56	0.48	125
T_g-7	120	0.44	90	0.48	199
T_g-7	240	0.40	140	0.48	310
T_g-7	480	0.44	192	0.48	423
T_g-17	60	3.25	74	0.48	160
T_g-17	120	3.25	121	0.48	259
T_g-17	240	3.00	277	0.48	485
T_g-17	480	3.00	301	0.48	644
T_g-27	60	7.08	312	0.32	2270
T_g-27	120	7.19	726	0.32	5290
T_g-27	240	7.05	1770	0.32	12900
T_g-27	480	7.37	2250	0.32	16400
T_g-37	60	10.3	1118	0.33	6887
T_g-37	120	10.3	1898	0.33	11639
T_g-37	240	10.0	4185	0.33	25780

occur anywhere in the material, i.e., in regions of high and low free volume, we use the mid-point T_g as the scaling temperature. In Figure 10, we compare the temperature dependence of τ_3 and R for PS, PPO, and 90/10 PS/PPO. Evidently, the hole sizes are largest by far for PPO, consistent with its much higher glass transition temperature.[36] Also, in the blend, in the temperature range $T_g - T > 30$°C, where the stress relaxation experiments were conducted, the hole sizes are larger than those in pure PS, consistent with the higher degree of molecular mobility manifested in the shorter stress relaxation times. This picture is amplified in Figure 11, where we show the temperature dependence of the fractional free volume h. The higher values of h in the blend reflect the fact that, in addition to an increase in the hole radius, there appears also to be an increase in the hole density, as measured by the oPs intensity I_3. These observations are consistent with estimates of the fractional free volume based on the approximate relation, $h = (V - 0.95V^*)/V$, suggested by Simha.[37] Here, V is the specific volume of the polymer, and V^* is a characteristic parameter which is computed from PVT data via statistical theory. Previously, we have shown[16] an excellent correlation between free volume values measured by oPs annihilation and those calculated from this equation. Using specific volume data of Yee[38] at 23°C, namely, V(PS) = 0.950 mL/g, and V(PPO) = 0.931 mL/g, and the theoretical values V^*(PS) = 0.9611 mL/g and V^*(PPO) = 0.865 mL/g, we obtain h(PS) = 0.039, and h(PPO) = 0.117. From Figure 11, the h/C values determined from oPs

Table VII Stretched Exponential Curves Fitting Results for PMMA/PEO (85/15) Blend

T_a (°C)	t_a (min)	E_o ($\times 10^8$ Pa)	τ (s)	β	$\langle\tau\rangle$ (s)
T_g-7	60	7.06	85	0.32	576
T_g-7	120	7.07	156	0.32	1060
T_g-7	240	7.00	252	0.32	1720
T_g-7	480	7.04	445	0.32	3030
T_g-17	60	9.06	414	0.29	4320
T_g-17	120	9.19	671	0.29	7000
T_g-17	240	9.26	1270	0.29	13300
T_g-17	480	9.00	3470	0.29	36200
T_g-27	60	10.3	1180	0.25	29100
T_g-27	120	10.3	2250	0.25	55600
T_g-27	240	10.0	6350	0.25	157000
T_g-27	480	10.1	9240	0.25	228000

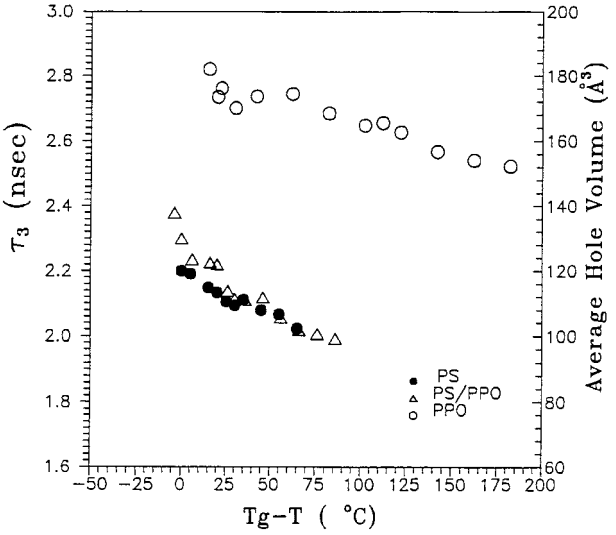

Figure 10 Orthopositronium lifetimes (τ_3) and average hole volumes $\langle V_h \rangle$ for PS, PPO, and PS/PPO (90/10) blend are compared at comparable aging temperature distances $T_g - T$.

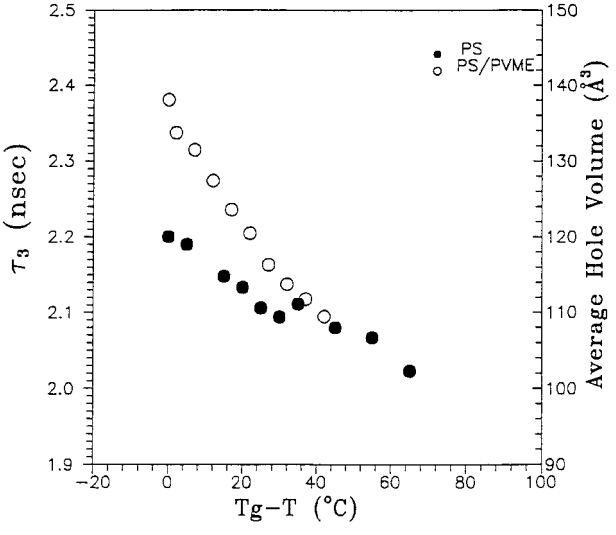

Figure 12 Orthopositronium lifetimes (τ_3) and average hole volumes $\langle V_h \rangle$ for PS homopolymer and PS/PVME (90/10) blend are compared at comparable aging temperature distances $T_g - T$.

data for PPO in the glass are approximately twice those for glassy PS, reasonably consistent with the calculated values, bearing in mind that the proportionality constant C is chemistry-dependent. It is also worth noting in Figure 11 that the increase in oPs free volume of PS on addition of PPO appears significantly smaller than expected on the grounds of additivity, which may reflect the fact that the excess volume of mixing is known to be negative.[38]

A similar situation is found when comparing oPs annihilation in the PS/PVME blend with that in pure PS. This is shown in Figure 12, where the temperature dependence of τ_3 and R is contrasted, and in Figure 13, where the behavior of h is exhibited. Again, in the temperature range of the stress relaxation experiments, the hole sizes and frac-

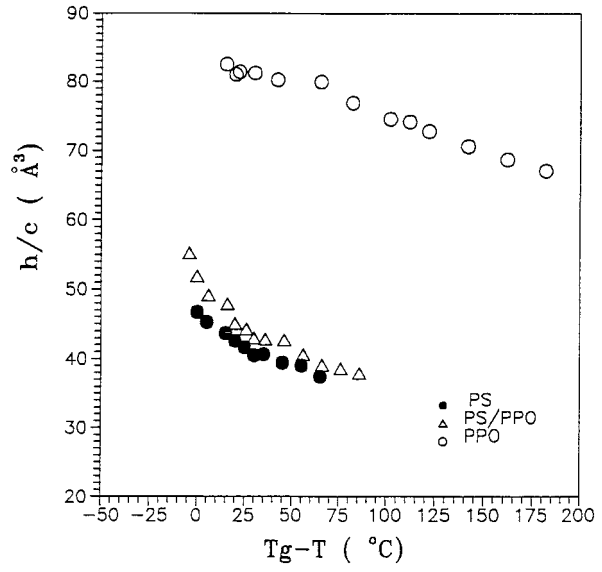

Figure 11 Apparent free volume fractions, $h/c = I_3\langle V_h \rangle$, computed from orthopositronium lifetimes. τ_3 and intensities I_3 are compared for PS, PPO, and PS/PPO (90/10) blend at equal aging temperature distances, $T_g - T$.

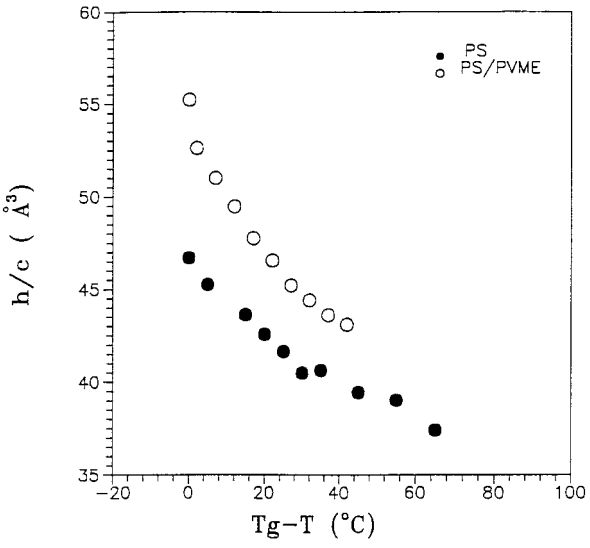

Figure 13 Apparent free volume fractions, $h/c = I_3\langle V_h \rangle$, computed from orthopositronium lifetimes. τ_3 and intensities I_3 are compared for PS homopolymer and PS/PVME (90/10) blend at equal aging temperature distances $T_g - T$.

tional free volume are each increased for the blend, consistent with the more rapid stress decay. In addition, the magnitude of the increase in R and h, relative to PS, is much larger for the PS/PVME blend than for PS/PPO, conforming with the fact that the rate of stress relaxation is also additionally enhanced in the former (cf Figs. 3 and 6).

Finally, in Figures 14 and 15, we show, respectively, the temperature dependence of τ_3 and R, and of h, for pure PMMA and the PMMA/PEO blend. Here, a quite different set of circumstances is found. From Figure 14, the hole sizes in the blend are smaller than in PMMA, particularly as the temperature is decreased into the glass. Even more striking, the fractional free volume in the blend is dramatically decreased, indicating a large decrease in hole density in the blend. Clearly, these results are in accord with the diminution in molecular mobility manifested in the stress relaxation experiments and suggest that the effect is indeed due to a more dense structure of the blend. A negative free volume deviation was earlier observed by oPs annihilation in miscible polyester blends[39] and in miscible blends of blends of tetramethyl bisphenol A polycarbonate/bisphenol A polycarbonate.[40]

CONCLUSIONS

Stress relaxation kinetics was studied in the glassy state for three polymer blends, PS/PPO, PS/PVME, and PMMA/PEO, dilute in one component, and compared with the corresponding behavior in the neat major component at equal temperature depths, $T_g - T$. For PS/PPO and PS/PVME, the relaxation times are shorter than for neat PS; for PMMA/PEO, the relaxation times are longer than for neat PMMA. In PS/PPO and PMMA/PEO, oPs annihilation measurements suggest that these differences are, respectively, due to an increase, and a decrease in the free volume of the blend relative to the neat major component. These conclusions are also supported by the observed changes in the β parameter, which describes the width of the stress relaxation time distribution. Specifically, in PS/PPO, β increases, i.e., the width of the relaxation spectrum decreases, characteristic of a weaker coupling of the relaxing elements to the surrounding matrix; in PMMA/PEO, β decreases, pointing to a stronger coupling. In PS/PVME, oPs annihilation data indicate an increase in free volume of the blend, consistent with its shorter stress relaxation times, but we also find a decrease in the β parameter. This suggests to us that the stress relaxation spectrum is broadened by the presence of sites of widely varying mobility, originating in the concentration fluctuations of the blend.

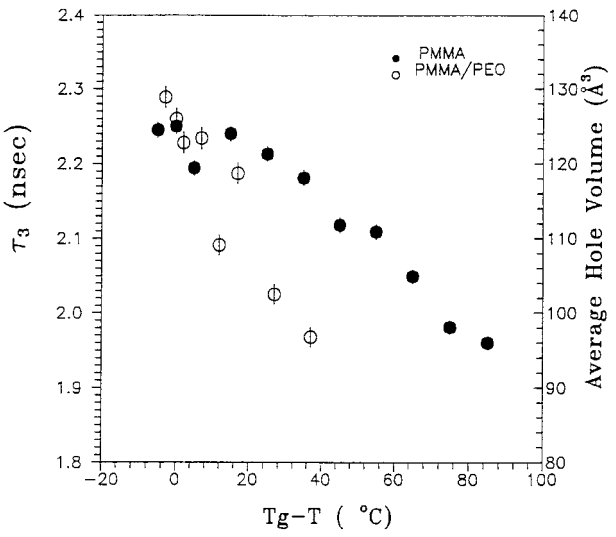

Figure 14 Orthopositronium lifetimes (τ_3) and average hole volumes $\langle V_h \rangle$ for PMMA homopolymer and PMMA/PEO (85/15) blend are compared at comparable aging temperature distances $T_g - T$.

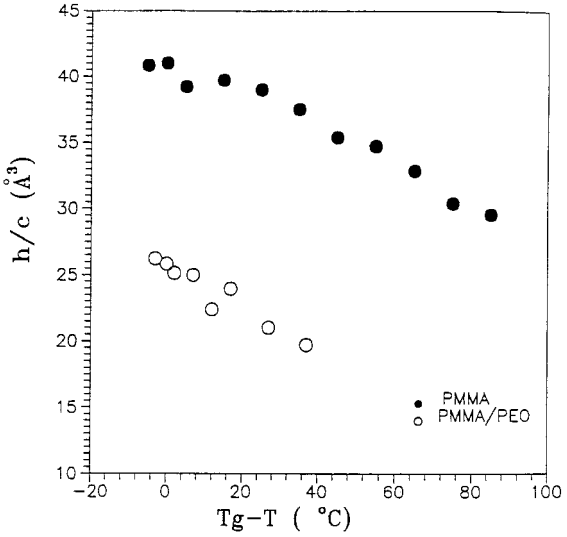

Figure 15 Apparent free volume fractions $h/c = I_3\langle V_h \rangle$, computed from orthopositronium lifetimes. τ_3 and intensities I_3 are compared for PMMA homopolymer and PMMA/PEO (85/15) blend at equal aging temperature distances, $T_g - T$.

We thank Professor Robert Simha for useful discussion and are grateful to the Edison Polymer Innovation Corporation for research support.

REFERENCES

1. L. C. E. Struik, *Physical Aging in Amorphous Polymers and Other Materials,* Elsevier Scientific, Amsterdam, 1978.
2. H. C. Booij and J. H. M. Palmen, *Polym. Eng. Sci.,* **18,** 781 (1978).
3. H. C. Booij and J. H. K. Minkhorst, *Polym. Eng. Sci.,* **19,** 579 (1979).
4. F. H. J. Maurer, J. H. M. Palmen, and H. C. Booij, *Rheol. Acta,* **24,** 243 (1985).
5. J. G. Victor and J. M. Torkelson, *Macromolecules,* **212,** 3694 (1988).
6. W. C. Yu, C. S. P. Sung, and R. E. Robertson, *Macromolecules,* **21,** 355 (1988).
7. E. F. Meyer, A. M. Jamieson, R. Simha, J. H. M. Palmen, H. G. Booij, and F. H. J. Maurer, *Polymer,* **31,** 243 (1990).
8. M. Shmorhun, A. M. Jamieson, and R. Simha, *Polymer,* **31,** 812 (1990).
9. J. S. Royal and J. M. Torkelson, *Macromolecules,* **25,** 4792 (1992).
10. J. R. Stevens, *Meth. Experim. Phys.,* **16A,** 371 (1980).
11. Y. C. Jean, *Microchem. J.,* **42,** 72 (1990).
12. Y. Kobayashi, W. Zheng, E. F. Meyer, J. D. McGervey, A. M. Jamieson, and R. Simha, *Macromolecules,* **22,** 2302 (1989).
13. J. E. Kluin, Z. Yu, S. Vleeshouwers, J. D. McGervey, A. M. Jamieson, and R. Simha, *Macromolecules,* **25,** 5089 (1992).
14. S. Vleeshouwers, J. E. Kluin, J. D. McGervey, A. M. Jamieson, and R. Simha, *J. Polym. Sci., Polym. Phys.,* **30,** 1429 (1992).
15. J. E. Kluin, Z. Yu, S. Vleeshouwers, J. D. McGervey, A. M. Jamieson, R. Simha, and K. Sommer, *Macromolecules,* **26,** 1853 (1993).
16. Z. Yu, U. Jahse, J. McGervey, A. M. Jamieson, R. Simha, *J. Polym. Sci., Polym. Phys.,* **32,** 2637 (1994).
17. Z. Yu, J. D. McGervey, A. M. Jamieson, and R. Simha, *Macromolecules,* **28,** 6268 (1995).
18. C. M. McCullagh, Z. Yu, A. M. Jamieson, J. Blackwell, and J. D. McGervey, *Macromolecules,* **28,** 6100 (1995).
19. J. Y. Cavaille, S. Etienne, J. Perez, L. Monnerie, and G. P. Johari, *Polymer,* **27,** 549, 686 (1986).
20. K. Pathmanathan and G. P. Johari, *J. Polym. Sci., Polym. Phys.,* **24,** 1587 (1986).
21. T. Ho, J. Mijovic, and C. Lee, *Polymer,* **32,** 619 (1991).
22. H. A. Schneider, H. Cantow, C. Wendland, and B. Weiklauf, *Makromol. Chem.,* **191,** 2377 (1990).
23. R. E. Wetton, W. J. McKnight, J. R. Fried, and F. R. Karasz, *Macromolecules,* **11,** 158 (1978).
24. S. Li, L. D. Charles, and J. C. W. Chien, *J. Appl. Polym. Sci.,* **43,** 1111 (1991).
25. P. Kirkegaard, N. J. Petersen, and M. Eldrup, *Riso National Laboratory, DIC 4000,* Roskilde, Denmark, Feb. 1989.
26. *Math View Professional*™ (*Software Operation Manual*), Brain Power, Inc., Calabasus, CA.
27. S. Matsuoka, G. Williams, G. E. Johnson, E. W. Anderson, and T. Furukawa, *Macromolecules,* **18,** 2652 (1985).
28. R. W. Rendell, J. J. Aklonis, K. L. Ngai, and G. R. Fong, *Macromolecules,* **20,** 1070 (1987).
29. A. F. Yee, R. J. Bankert, K. L. Ngai, and R. W. Rendell, *J. Polym. Sci., Polym. Phys.,* **26,** 2463 (1988).
30. R. Simha, J. G. Curro, and R. E. Robertson, *Polym. Sci. Eng.,* **24,** 1071 (1984).
31. J. R. Lefebvre, R. S. Porter, and G. D. Wignall, *Polym. Sci. Eng.,* **27,** 423 (1987).
32. J. I. Marcos, E. Orlandi, and G. Zerbi, *Polymer,* **31,** 1899 (1990).
33. R. H. Colby, *Polymer,* **30,** 1275 (1989).
34. S. Wu, *J. Polym. Sci., Polym. Phys.,* **25,** 557, 2511 (1987).
35. J. A. Zawada, M. Y. Caroline, G. F. Gerald, R. H. Colby, and T. E. Long, *Macromolecules,* **25,** 2896 (1992).
36. R. Simha and T. Somcynski, *Macromolecules,* **2,** 324 (1969).
37. R. Simha, personal commun., 1996.
38. A. F. Yee, *Polym. Sci. Eng.,* **17,** 213 (1977).
39. M. D. Zipper, G. P. Simon, M. R. Tant, J. D. Small, G. M. Stack, and A. J. Hill, *Polym. Intl.,* **36,** 127 (1995).
40. J. Liu, Y. C. Jean, and H. Yang, *Macromolecules,* **28,** 5774 (1995).